Eigenvalue spectrum of the Frobenius-Perron operator near intermittency

Z. Kaufmann
Institute for Solid State Physics, Eötvös University, P.O. Box 327, H-1445 Budapest, Hungary

H. Lustfeld
Institut für Festkörperforschung, Forschungszentrum Jülich, D-52425 Jülich, Germany

J. Bene
Institute for Solid State Physics, Eötvös University, P.O. Box 327, H-1445 Budapest, Hungary
(Received 9 March 1995; revised manuscript received 7 September 1995)

The spectral properties of the Frobenius-Perron operator of one-dimensional maps are studied when approaching a weakly intermittent situation. Numerical investigation of a particular family of maps shows that the spectrum becomes extremely dense and the eigenfunctions become concentrated in the vicinity of the intermittent fixed point. Analytical considerations generalize the results to a broader class of maps near and at weak intermittency and show that one branch of the map is dominant in the determination of the spectrum. Explicit approximate expressions are derived for both the eigenvalues and the eigenfunctions and are compared with the numerical results.

PACS number(s): 05.45.+b

I. INTRODUCTION

Correlation functions play an important role in the characterization of chaotic systems. In certain classes of systems they decay exponentially. Cases when it is proven are Axiom A systems [1–3], mixing maps [4], and maps that are analytic on a set of rectangles [5]. It is generally believed that hyperbolic systems usually exhibit an exponential correlation decay, although the rigorous proof of this can be quite a difficult task in particular cases [6]. On the other hand, there are similarly important classes of systems where the decay of correlations is slower than exponential. Such a behavior has been found in intermittent one-dimensional maps [7] and in Hamiltonian systems with mixed phase space [8]. Intermittency, the alternation of almost regular and chaotic motion, can precede the birth of a pair of stable-unstable fixed points or periodic orbits (tangent bifurcation) [9,10]. It can be associated with a marginally unstable fixed point [7,11–14] or the marginal behavior at the boundary of an island in general Hamiltonian systems [8]. It can also arise when a chaotic attractor becomes unstable due to crises [15], effect of noise, or driving of another attractor [16,17]. Intermittency is known to possess several special properties. The spectrum of the Rényi entropies of intermittent systems shows a phase-transition-like behavior [13,18–21], and the decay properties of their truncated entropies, complexity and the dynamical fluctuations also differ from those of expanding maps [12,20,22–25]. The kind of intermittency we study is due to a marginally unstable fixed point [11,7,12–14]. The vicinity of the fixed point is visited by typical trajectories and the time needed to leave this vicinity scales with a power of the distance from the fixed point instead of the logarithm, as for an unstable fixed point. Depending on the actual map there can even exist a smooth invariant density to which initial densities converge, as in the case of our example. This case is called weak intermittency; otherwise, we talk about strong intermittency [7].

The decay of correlations may be related to the spectral properties of the Frobenius-Perron operator describing the time evolution of the probability density given in the phase space of the system in question. The rough picture is that the largest eigenvalue is unity (except for transient chaos [26], which is not to be treated here) and the corresponding eigenfunction is related to the natural measure, while the leading asymptotics of the correlation decay is related to a spectral gap between the largest eigenvalue and the rest of the spectrum. Note that in two-dimensional systems or higher, even in hyperbolic cases the direct study of the spectrum of the Frobenius-Perron operator involves a series of difficulties, related to both the suitable definition of the Frobenius-Perron operator and the relevant function space in which the eigenvalue problem is to be solved.

In the case of one-dimensional maps the Frobenius-Perron operator takes the form $L\varphi(x) = \sum_{z:f(z)=x} \frac{\varphi(z)}{|f'(z)|}$. Here the sum goes over the preimages z of x. The existence of a unique invariant density (belonging to eigenvalue $\lambda_0 = 1$) is proven for expanding piecewise C^2 maps [27] and fully developed maps with a negative Schwarzian derivative [28]. If a unique ergodic measure exists the correlation function can be expressed in terms of the Frobenius-Perron operator. If the spectrum is discrete eigenvalues λ_n and eigenfunctions φ_n may be used to explore the time evolution of an initial probability density $\varphi(0,x)$. Then the decay of correlations and the convergence of $\varphi(t,x)$ towards the invariant density is governed by λ_1 (where $\lambda_0 > |\lambda_1| \geq |\lambda_2| \geq \ldots \geq |\lambda_n| \geq \ldots$).

The relation between the spectral properties and the correlation decay becomes much more complex if the lat-

1063-651X/96/53(2)/1416(6)/$06.00

ter one is slower than exponential. In such a case, arising typically in intermittent systems, the largest eigenvalue must be an accumulation point of the spectrum. The standard methods [3,29–32] developed for determining the eigenvalues of operators similar to the Frobenius-Perron operator cannot be used to determine the nonleading eigenvalues when the system is close to an intermittent situation. A direct study of the spectrum of generalized Frobenius-Perron operators in case of intermittency can be found in Ref. [33]. Working in the space of functions with bounded variation a nonzero essential spectral radius [34] is obtained, which reaches λ_0 for the case of L [33]. A study of the spectrum for intermittency that precedes tangent bifurcation is presented in [35].

Our motivation has been to calculate the spectral properties near and at intermittency and to establish their link to the correlation decay. In the present paper we concentrate on the first task, while the derivation of the correlation functions will be presented elsewhere [36]. In order to avoid the difficulties arising in higher dimensional systems we consider piecewise analytic one-dimensional maps and choose the function space of real analytic functions. Note that the methods and the function space used here are different from those in Ref. [33], and allow us a more detailed description. The paper is organized as follows. In Sec. II we study the spectral properties of the Frobenius-Perron operator numerically in a family of fully developed chaotic maps [37,38], where the parameter is tuned up to weak intermittency. Some aspects of the numerical work are discussed in Appendix A. Section III contains the analytical results, which are valid for a wider class of maps. Details of the calculation are given in Appendix B.

II. MODEL AND NUMERICAL CALCULATION

Our model is the piecewise parabolic map [38]. This is probably the simplest dynamical system that can show intermittency. The general form of the map is

$$f_r(x) = \frac{1 + r - \sqrt{(1-r)^2 + 4r|1-2x|}}{2r} . \qquad (1)$$

It maps the interval $[0,1]$ twice onto itself for every value of the parameter r in the interval $[-1,1]$. Its name comes from the fact that its inverse has parabolic branches. The point $x=0$ is a fixed point that becomes marginal in the intermittent case $r=1$ [38,39,7]. For the other special case $r=0$ we obtain the uniformly expanding tent map. A special property of the piecewise parabolic map is that the stationary probability density has a simple form [38], $p_r(x) = 1 + r(1-2x)$. This is still normalizable for $r=1$, which means that the map possesses weak intermittency. Note that the average Liapunov exponent is positive.

In order to study the eigenvalue spectrum of the Frobenius-Perron operator we derive a matrix representation on the basis of the Legendre polynomials P_k. After normalization $Q_k(x) = \sqrt{k+1/2}P_k(x)$ these polynomials form a complete orthonormal system on the interval $[-1,1]$. In order to use them we have to transform the map and this basis to the same interval.

In the case of our model the action of the Frobenius-Perron operator on an arbitrary function $\varphi(x)$ can be given by

$$L\varphi(x) = [\varphi(F_1(x)) + \varphi(F_2(x))]\, |F_2'(x)| , \qquad (2)$$

where $F_{1,2}(x) = \frac{1}{2} \mp \left(\frac{1}{2} - \frac{1+r}{2}x + \frac{r}{2}x^2\right)$ stands for the inverse branches of the map.

Expanding the function $\varphi(x)$ in terms of $Q_k(x)$ as $\varphi(x) \approx \sum_{k=0}^{\infty} b_k Q_k(x)$ we obtain the (infinite) matrix representation of the Frobenius-Perron operator,

$$L\varphi(x) = \sum_{k,l=0}^{\infty} L_{lk} b_k Q_l(x) , \qquad (3)$$

where the matrix elements L_{lk} are of the form $L_{lk} = \int_{-1}^{1} Q_l(x) L Q_k(x)\, dx$. In the numerical calculation we have truncated this matrix confining the indices between 0 and N. The integrals have been evaluated by numerical integration. Exploiting the symmetry of the map the matrix size has been effectively reduced by a factor of 2. Then the eigenvalue spectrum $\lambda_n^{(N)}$, $n = 0,1,2,\ldots$ of the matrix has been determined. It was quite remarkable that the eigenvalues turned out to always be positive real numbers. This calculation was performed for different values of the parameters r and N. Figure 1 shows the spectrum as a function of the parameter r at two different values of N. The solid parts of the curves in Fig. 1 correspond to cases where, at the given value of N, the precision of the eigenvalues has reached 0.003 (which is approximately the resolution of the figure). The precision was determined by comparing results for different values of N.

It is seen that all the eigenvalues λ_n with fixed n tend to value 1 for $r \to 1$. On the other hand we find that near any fixed λ value the density of the eigenvalues increases, suggesting a continuous spectrum at intermittency. The eigenfunctions of the operator also show a

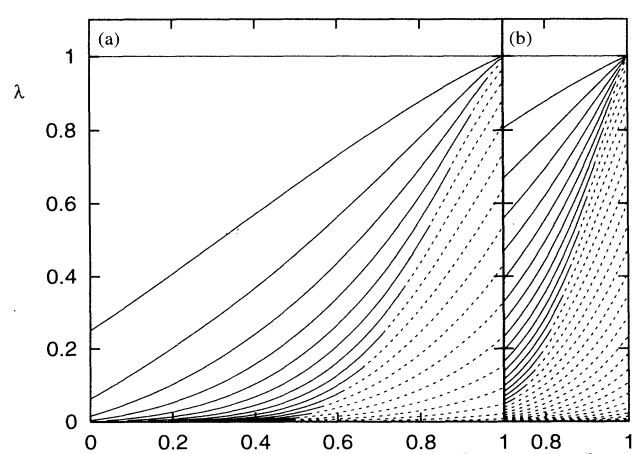

FIG. 1. Eigenvalues of the Frobenius-Perron operator L for the piecewise parabolic map with maximal matrix index (a) $N=40$, (b) $N=80$. Solid lines: precision higher than 0.003; dashed lines: precision lower than 0.003.

remarkable behavior when approaching the intermittent case $r = 1$. Apart from the first one, they become more and more concentrated in the vicinity of the fixed point (see Fig. 2). That means, the limiting eigenfunctions are singular. One might expect the strange case that the eigenvalue $\lambda_0 = 1$ becomes infinitely degenerate in the space of analytic functions. This is avoided since the eigenfunctions become singular in the limit. At the same time the tails of the eigenfunctions outside the vicinity of the fixed point are smooth functions and become more and more similar to the invariant density $p(x)$ (see inset in Fig. 2). In fact, with a suitable normalization they converge to $p(x)$.

It has been observed that for $r \leq 0.9$ the eigenvalues converge quite fast when increasing the value of N. Going closer to the case $r = 1$ the convergence becomes slower and the limiting eigenvalues get closer to the largest one ($\lambda_0 = 1$). In the case $r = 1$ the eigenvalues converge to unity, but slower than exponentially. At the same time the eigenvalues with higher index converge slower, consequently the closer r is to unity the less eigenvalues are precise. Its reason is twofold. On the one hand, the spectrum becomes denser and denser when approaching the intermittent case, which certainly leads to numerical problems. On the other hand, the eigenfunctions $\varphi_n(x)$ close to the intermittent situation after suitable conjugation can be well approximated by powers x^{n-1}. As is explained in Appendix A, this leads to the problem that only a few eigenvalues and eigenfunctions can be obtained numerically.

III. ANALYTICAL RESULTS

We can understand the behavior of the spectrum near the intermittent case by keeping only the term of the Frobenius-Perron operator $L\varphi(x) = \sum_{z:f(z)=x} \frac{\varphi(z)}{|f'(z)|}$

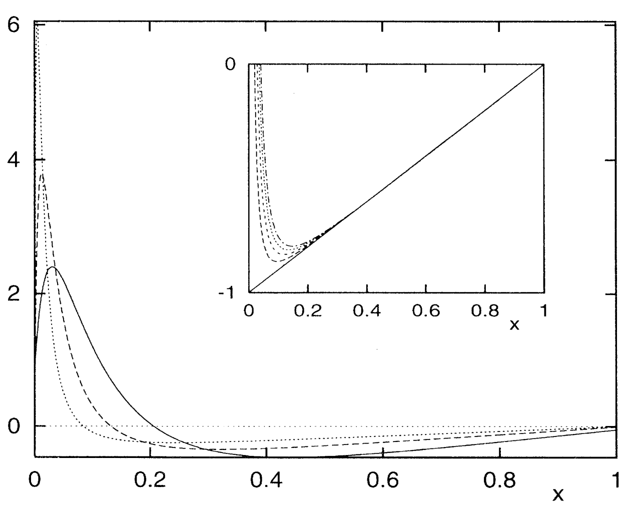

FIG. 2. Eigenfunction φ_2 for $r = 0.9$ (solid line), $r = 0.97$ (dashed line), and $r = 0.99$ (dotted line). Inset: The eigenfunctions φ_0 (solid line), φ_1 (long dashes), φ_2 (short dashes), φ_3 (dotted line), and φ_4 (dashed-dotted line), for $r = 0.999$ with different normalization.

that corresponds to the lower inverse branch. This branch contains the intermittent fixed point. (We shall denote the corresponding operator by L_1, while the operator containing the upper inverse branch of the map will be denoted by L_2.) The first explanation is the following. The numerical results show that the eigenfunctions, except for the invariant density $p(x)$, are concentrated in the vicinity of the fixed point. Therefore the most important region is this neighborhood. The contribution of L_2 comes from the rightmost piece of the interval [0,1], while this piece is reached from the neighborhood of the maximum in one iteration. At the same time the eigenfunctions are smooth and [except for $p(x)$] have quite a low value there compared to the vicinity of the fixed point. Therefore the contribution of the upper branch is small and is a slowly varying function. So we first study L_1 and later we return to the full Frobenius-Perron operator to estimate the effect of the upper branch. The considerations are quite general; we assume that the map is single-humped, that special properties of the map exist at the endpoints and the maximum, and that the map is smooth and expanding everywhere else.

Without restricting generality we let the map act on the interval $[0, 1]$ so that the fixed point is at $x = 0$. We assume that the map satisfies the following formulas such as model (1) does:

$$f(x) = \begin{cases} (1+\varepsilon)x + ax^2 + O(x^3) & \text{if } x \ll 1 \quad (4) \\ d(1-x) + O((1-x)^2) & \text{if } 1-x \ll 1\,, \quad (5) \end{cases}$$

$$F_{1,2}(x) = \hat{x} \mp [g_{1,2}\varepsilon(1-x) + h_{1,2}(1-x)^2] + O((1-x)^3) \quad \text{if } 1-x \ll 1\,, \tag{6}$$

where $\hat{x}$ is the location of the maximum, $\varepsilon, a, d, g_{1,2}, h_{1,2}$ are suitable positive constants, and $F_{1,2}$ are the inverse branches of $f(x)$. For $\varepsilon \to 0$ keeping $a, d, g_{1,2}, h_{1,2}$ fixed we are approaching the intermittent situation. The eigenvalue equation for L_1 takes the form

$$\lambda\varphi(f(x)) = \frac{\varphi(x)}{|f'(x)|}\,, \quad 0 \leq x \leq \hat{x}\,. \tag{7}$$

We can solve it in the neighborhood of the origin by introducing $\omega(x) = \ln\varphi(x)$. Since $f(x) - x$ is small when we are close to the intermittent case, $\omega(f(x)) - \omega(x)$ can be approximated by the linear term of Taylor expansion. Then one obtains

$$\omega'(x) = -\frac{\ln f'(x) + \ln\lambda}{f(x) - x} + O(\varepsilon^2). \tag{8}$$

Substitution of (4) and integration yields

$$\varphi(x) \approx c\frac{x^{\nu(\lambda)}}{\left(x + \frac{\varepsilon}{a}\right)^{\nu(\lambda)+2}}\,, \tag{9}$$

where $\nu(\lambda) = \frac{-\ln\lambda}{\varepsilon} - 1 + \frac{\varepsilon}{2}$. Let us restrict ourselves to the case of analytic eigenfunctions; that means $\nu(\lambda) = n - 1$, where n is a positive integer. Then

$$\varphi_n(x) \approx c\frac{x^{n-1}}{(x + \frac{\varepsilon}{a})^{n+1}}\,. \tag{10}$$

The corresponding eigenvalue is obtained from the expression below (9) as $\lambda_n \approx e^{-n\varepsilon}$.

It is interesting to see that even the exact eigenvalues of L_1 [see (7)] for a not necessarily small ε can be obtained from the stability of the fixed point. The reason is the following. If we know the eigenfunction $\varphi(x)$ in any small neighborhood V_0 of the fixed point, then by (7) we can determine it in the image V_1 of this interval. Repeating this procedure, say k times, the part of the interval V_k lying outside the previous one V_{k-1} will be mapped outside V_k . Hence we can find the eigenfunction satisfying (7) in $[0,\hat{x}]$. For small enough neighborhood V_0 the function $f(x)$ can be approximated linearly, which yields eigenfunctions x^{n-1} and eigenvalues

$$\lambda_n = (1+\varepsilon)^{-n} \ , \quad n = 1,2,\ldots \ . \qquad (11)$$

Moreover, these are the exact eigenvalues of L_1, since the relative precision of the linear approximation can be arbitrarily increased by shrinking the interval V_0. However, for the determination of the eigenfunctions the quadratic term in (4) is important.

After these considerations we can estimate the effect of the upper inverse branch of the map. The eigenvalue equation may be written as

$$\lambda f_1'(x)\varphi(f(x)) = \varphi(x) + \chi(x) \ , \qquad (12)$$

$$\chi(x) = \varphi(F_2(f(x)))f_1'(x)F_2'(f(x)) \ . \qquad (13)$$

It is seen from Eq. (10) that very close to the fixed point the eigenfunction starts as $\varphi_n(x) \approx \beta x^{n-1}$ (we do not fix the normalization here, β may contain a power of ε) and it is concentrated in a region of width of order ε. We assume that the eigenfunction gets small corrections compared to Eq. (10). After estimating the value of φ_n and writing down power-series forms for it in the neighborhood of $x = 0$ and $\hat{x}$, we obtain results for λ_n and coefficients of the expansion $\varphi_n(x) = \sum_{k=0}^{\infty} \beta_k x^k$:

$$\beta_m = O(\beta\varepsilon^{n-m}) \ \text{if} \ m < n-1 \ , \qquad (14)$$

$$\lambda_n = (1+\varepsilon)^{-n} + O(\varepsilon^2) \ . \qquad (15)$$

The actual value of the correction depends on the shape of the map but its order of magnitude does not. The order of the correction in (15) was also shown by the numerical results for the map (1) for the $n = 1,2,3$ eigenvalues. For the perturbation of the eigenfunction [see Eq. (14)] the case $m = 0$ shows that the eigenfunction is shifted, and the ratio of this shift β_0 and the maximum is of order ε. This was numerically verified for $n = 2,3$ (see the nonzero starting value in Fig. 3). The value β_1 gives the initial slope of the eigenfunction at the fixed point. β_1 can be compared to the slope $O(\beta\varepsilon^{n-2})$ of the straight line connecting the origin and the maximum of φ_n. Their ratio is also proportional to ε, what was numerically checked for $n = 3$.

It is important to mention that not only values of λ_n, β_0, and β_1 show good agreement between the analytic and numeric results. The shape of the eigenfunction itself agrees very well, too. The agreement is surprisingly good for $r = 0.999$. Figure 3 also supports the above estimations, namely, that the deviation, which is due to the effect of the upper branch, is proportional to ε. One should notice that we did not get the eigenvalue $\lambda_0 = 1$ this way. The reason is that for $n = 0$ the eigenfunction is not concentrated in the vicinity of the fixed point, as indicated in the beginning of this section. This means the contribution $\chi(x)$ of the upper inverse branch of the map is not negligible in this case.

In the above estimation of the effect of the second branch, n was assumed to be constant. However, the effect of L_2 remains also small in the limit $r \to 1$ when n tends to infinity in such a way that λ_n is kept constant. This can be realized using a series of r_n values which satisfy $\lambda_n(r_n) = \lambda$. The effect of L_2, i.e., the difference $\delta\lambda_n$ of analytic eigenvalues (11) for L_1 and numeric eigenvalues for L, was determined for several values of n and

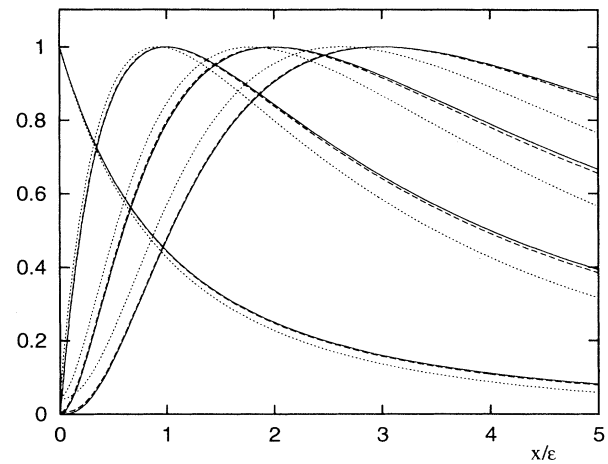

FIG. 3. Comparison of eigenfunctions φ_1, φ_2, φ_3, and φ_4 of L_1 obtained analytically (solid lines) with corresponding eigenfunctions of L calculated numerically for $r = 0.99$ (dotted lines) and for $r = 0.999$ (dashed lines) in the vicinity of the fixed point. For identification of the curves we note that $\varphi_1 < \varphi_2 < \varphi_3 < \varphi_4$ at the right edge of the figure.

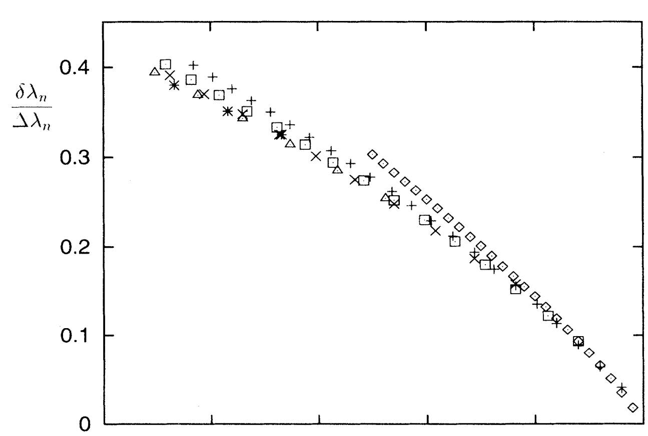

FIG. 4. Effect of the second branch on the eigenvalues compared to the eigenvalue spacing in function of λ and n. $\Diamond$, $n = 1$; $+$, $n = 2$; $\square$, $n = 3$; $\times$, $n = 4$; $\triangle$, $n = 5$; $*$, $n = 6$.

r. Since the spacing $\Delta\lambda_n = \lambda_n - \lambda_{n+1}$ of the eigenvalues decreases in the limit the relative precision $\delta\lambda_n/\Delta\lambda_n$ is important. Figure 4 shows that this ratio is roughly constant in function of n (depends on λ only) when it is considered as a function of n and λ, and it is small for $\lambda \approx 1$. According to these numerical findings one may assume that also the expression (10) for the eigenfunctions is valid with a fixed precision in the limit $\varepsilon \to 0$ for fixed λ. Therefore an approximating eigenfunction can be obtained for the intermittent case $r = 1$ as the limit of (10), which can also be calculated using (9), the expression of $\nu(\lambda)$ and keeping λ fixed. This way one obtains

$$\varphi_\lambda(x) \approx A_\lambda \frac{1}{x^2} e^{-\frac{|\log \lambda|}{ax} + 2ax} , \tag{16}$$

while the spectrum is found to be continuous.

ACKNOWLEDGMENTS

The authors thank T. Tél for reading the manuscript and making several valuable remarks. This work has been supported by the International Relations Offices of Germany and Hungary, Project No. X231.3 and by the Hungarian Academy of Sciences under Grant Nos. OTKA 2090 and OTKA F.4286. Two of the authors (J.B. and Z.K.) are grateful for the hospitality of the Institut für Festkörperforschung, Forschungszentrum Jülich GmbH, where part of the work has been done. One of the authors (H.L.) is grateful for the hospitality of the Institute for Solid State Physics, Eötvös University Budapest, where another part of the work has been done.

APPENDIX A: REPRESENTING THE EIGENFUNCTIONS ON AN ORTHONORMAL BASIS

In this appendix we explain why an orthonormal basis is not well suited to get many eigenvalues correctly near an intermittent state. This is easier to see after applying the following conjugation to the piecewise parabolic map:

$$y = h(x) = \frac{x}{x + \frac{\varepsilon}{a}} \left(1 + \frac{\varepsilon}{a}\right) . \tag{A1}$$

Then the eigenfunctions of the map can be well approximated by powers $\{y^n\}$ near intermittency. Therefore $\langle \Phi_m | L | y^n \rangle$ is a good matrix representation of L, where $\{\Phi_n\}$ is the adjoint basis to $\{y^n\}$.

Using an orthonormal basis $\{q_n(y)\}$ the matrix elements $L_{nm} = \langle q_n | L | q_m \rangle$ can be obtained by the following transformation:

$$\langle \Phi_m | L | y^n \rangle = \sum_{l,k} W^{-1}_{mk} L_{kl} W_{ln} , \tag{A2}$$

where $W_{nm} = \int_0^1 q_n(y) y^m \, dy$. How many eigenvalues we can get correctly depends on how weakly conditioned the matrix W_{nm} is.

In our case $\{q_n(x)$ is the normalized Legendre polynomial transformed to $[0,1]\}$ the matrix elements can be calculated analytically using Rodrigues formula and applying partial integration:

$$W_{nm} = \begin{cases} \dfrac{\sqrt{2n+1}(m!)^2}{(m-n)!(m+n+1)!} & \text{for } n \le m \\ 0 & \text{for } n > m. \end{cases} \tag{A3}$$

The maximum number N_{max} of eigenvalues and eigenvectors that can be reliably computed can be approximately read off from the singular value decomposition representing a matrix W as $W_{i,j} = U_{il} D_{ll} V^T_{l,j}$. Here U and V are orthogonal $n \times n$ matrices and D is diagonal one with the property $D_{ii} \ge D_{jj} \ge 0$ for $i < j$. We have determined N_{max} from the condition

$$D_{N_{max},N_{max}} > \delta, \;\; D_{N_{max}+1,N_{max}+1} \le \delta, \tag{A4}$$

with two different choices for δ (10^{-5} and 10^{-10}). It is seen in Table I, that N_{max} increases slowly with increasing n. Therefore we conclude that close to intermittency the shifted Legendre polynomials represent a good basis to determine the first few eigenvalues and eigenfunctions. Beyond that they are expected to produce misleading results. We surmise that these conclusions are intrinsic for any orthogonal basis, since the matrix W is nearly degenerate. This corresponds to the fact that the basis functions y^n are nearly parallel for large n when angles are defined through the usual $\mathcal{L}_2$ norm.

APPENDIX B: EFFECT OF THE UPPER INVERSE BRANCH

To obtain estimations (14) and (15) we start from Eqs. (12) and (13). It follows that the order of the maximum value of $\varphi(x)$ is $\beta\varepsilon^{n-1}$. The numerical calculation not only supports these estimates but shows that the function outside that region is smooth and slowly varying. The integral of the eigenfunction should be zero, since it should be orthogonal to the first left eigenfunction of L. At the same time its integral in the above mentioned region near 0 is of order $\beta\varepsilon^n$; hence, it should be of the same order around the position $\hat{x}$ where f has its maximum. Thus the Taylor expansion $\varphi(x) = \sum_{k=0}^{\infty} \hat{c}_k (x - \hat{x})^k$ possesses coefficients of order $\beta\varepsilon^n$ at most, $\hat{c}_k = O(\beta\varepsilon^n)$. Going to the iterate of $\hat{x}$ we apply Eq. (12) for $x \approx f(\hat{x}) = 1$. Using Eq. (6) we obtain estimation for the Taylor series around the point $x = 1$. The second term of (12) connects it to $\varphi(x)$ around $x = 0$. Since the expressions $F_2(f(x))$ and $f(x)$ in (13) start linearly for $x \approx 0$ the coefficients in the expansions $\chi(x) = \sum_{k=0}^{\infty} c_k x^k$ and $\varphi(x) = \sum_{k=0}^{\infty} \tilde{c}_k (1 - x)^k$ are of the same order of magni-

TABLE I. Values of N_{max} in function of n for different δ.

n	$\delta = 10^{-5}$	$\delta = 10^{-10}$
5	5	5
10	8	10
20	10	16
50	12	21
100	14	24
500	18	32
1000	20	35

tude: $c_0, \tilde{c}_0 = O(\beta\varepsilon^{n+1})$, $c_k, \tilde{c}_k = O(\beta\varepsilon^n)$, $k > 0$.

Returning to the neighborhood of the intermittent fixed point we apply (12) for $x \approx 0$. We describe the corrected eigenfunction by the expansion $\varphi(x) = \sum_{k=0}^{\infty} \beta_k x^k$, where $\beta_k,\ k < n-1$ are small and $\beta_{n-1} \approx \beta$, which ensures that the eigenfunction gets small correction. Substituting the expansions for $\varphi(x), \chi(x)$ and (4) into (12), expanding the powers and collecting terms proportional to x^m we obtain

$$\lambda \sum_{k=Int(\frac{m}{2})}^{m-1} b_{m,k}\alpha^{m-k}(1+\varepsilon)^{2k+1-m}\beta_k + \left[\lambda(1+\varepsilon)^{m+1} - 1\right]\beta_m = c_m + \sum_{k=0}^{m-2} O(\beta_k)\ , \qquad \text{(B1)}$$

where $b_{m,k} = \left[\binom{k}{m-k} + 2\binom{k}{m-k-1}\right]$, and $\binom{p}{q} = 0$ if $q > p$ or $q < 0$. Using this equation and the estimations for c_k it can be shown recursively that $\beta_m = O(\beta\varepsilon^{n-m})$, if $m < n-1$. For $m = 0$ only the term containing β_m remains on the left-hand side. Since the eigenvalue (11) is expected to get small correction the coefficient of β_m in (B1) is of order ε. This yields $\beta_0 = O(\beta\varepsilon^n)$. For $m > 0$ the sum in (B1) is not suppressed by c_m, so we get $\beta_m = O(\varepsilon^{-1}\beta_{m-1})$, which proves our statement for β_m. However, for $m = n-1$ the eigenvalue (11) would give zero for the coefficient of β_m; therefore, this coefficient depends strongly on the perturbation of λ. At the same time in the case $m = n-1$ the order of $\beta_m = \beta_{n-1} \equiv \beta$ is known; hence, this case determines the corrected value of λ with the help of β_m: $\lambda_n = (1+\varepsilon)^{-n} + O(\varepsilon^2)$.

---

[1] R. Bowen, *Equilibrium States and the Ergodic Theory of Anosov-diffeomorphisms*, Lecture Notes in Mathematics Vol. 470 (Springer, Berlin, 1975).
[2] M. Pollicott, Invent. Math. **81**, 413 (1985).
[3] D. Ruelle, J. Stat. Phys. **44**, 281 (1986).
[4] D. Ruelle, *Thermodynamic Formalism*, Encyclopedia of Mathematics and its Applications Vol. 5 (Addison-Wesley, Reading, MA, 1978).
[5] H.H. Rugh, Nonlinearity **5**, 1237 (1992).
[6] C. Liverani, J. Stat. Phys. **78**, 1111 (1995).
[7] S. Grossmann and H. Horner, Z. Phys. B **60**, 79 (1985).
[8] P. Grassberger and H. Kantz, Phys. Lett. **113A**, 167 (1985).
[9] P. Manneville and Y. Pomeau, Physica D **1**, 219 (1980).
[10] Y. Pomeau and P. Manneville, Commun. Math. Phys. **74**, 189 (1980).
[11] P. Manneville, J. Phys. (Paris) **41**, 1235 (1980).
[12] P. Szépfalusy and G. Györgyi, Phys. Rev. A **33**, 2852 (1986).
[13] P. Szépfalusy, T. Tél, A. Csordás, and Z. Kovács, Phys. Rev. A **36**, 3525 (1987).
[14] H. Okamoto, H. Mori, and S. Kuroki, Prog. Theor. Phys. **79**, 581 (1988).
[15] C. Grebogi, E. Ott, and J.A. Yorke, Phys. Rev. Lett. **48**, 1507 (1982).
[16] N. Platt, E.A Spiegel, and C. Tresser, Phys. Rev. Lett. **70**, 279 (1993).
[17] A. Čenys and H. Lustfeld (unpublished).
[18] A. Csordás and P. Szépfalusy, Phys. Rev. A **39**, 4767 (1989).
[19] J. Bene, P. Szépfalusy, and A. Fülöp, Phys. Rev. A **40**, 6719 (1989).
[20] Z. Kaufmann and P. Szépfalusy, Phys. Rev. A **40**, 2615 (1989).
[21] P. Szépfalusy, T. Tél, and G. Vattay, Phys. Rev. A **43**, 681 (1991).
[22] P. Szépfalusy, in *Synergetics, Order and Chaos*, edited by M. Velarde (World Scientific, Singapore, 1988), pp. 685–697.
[23] P. Szépfalusy, Phys. Scr. **T25**, 226 (1989).
[24] P. Gaspard and X.-J. Wang, Proc. Natl. Acad. Sci. USA **85**, 4591 (1988).
[25] X.-J. Wang, Phys. Rev. A **40**, 6647 (1989).
[26] T. Tél, in *Directions in Chaos*, edited by Hao Bai-Lin (World Scientific, Singapore, 1990), Vol. 3.
[27] A. Lasota and J.A. Yorke, Trans. Am. Math. Soc. **186**, 481 (1973).
[28] M. Misiurewicz, in *Chaotic Behavior of Deterministic Systems*, edited by G. Ioos, R.H.G. Helleman, and R. Stora (North-Holland, Amsterdam, 1983).
[29] P. Szépfalusy and T. Tél, Phys. Rev. A **34**, 2520 (1986).
[30] T. Tél, Phys. Rev. A **36**, 2507 (1987).
[31] R. Artuso, E. Aurell, and P. Cvitanovic, Nonlinearity **3**, 325 (1990); **3**, 361 (1990).
[32] F. Christiansen, G. Paladin, and H.H. Rugh, Phys. Rev. Lett. **65**, 2087 (1990).
[33] T. Prellberg, dissertation, Virginia Polytechnic Institute and State University, 1991 (unpublished).
[34] D. Ruelle, Commun. Math. Phys. **125**, 239 (1989).
[35] V. Baladi, J-P. Eckmann, and D. Ruelle, Nonlinearity **2**, 119 (1989).
[36] H. Lustfeld, J. Bene, and Z. Kaufmann (unpublished).
[37] G. Györgyi and P. Szépfalusy, J. Stat. Phys. **34**, 451 (1984).
[38] G. Györgyi and P. Szépfalusy, Z. Phys. B **55**, 179 (1984).
[39] P.C. Hemmer, J. Phys. A **17**, L247 (1984).